Bond percolation on a finite lattice: Critical behavior of the $(1+\epsilon)$-state Potts model

Joseph Rudnick and Jacob Morris*
Department of Physics, University of California, Los Angeles, Los Angeles, California 90024-1547

George Gaspari
Department of Physics, University of California, Santa Cruz, Santa Cruz, California 95064
(Received 28 June 1993)

The continuous n-state Potts model is reinvestigated. The partition function is cast in a form allowing the limit, $n \to 1$, to be taken prior to perturbation-theoretical expansions. Proceeding in this way, we free the theory of pathologies known to plague other approaches. Several alternatives are presented for a Feynman-diagrammatic expansion of the theory, two of which are identical to those utilized in previous analyses of the mdoel. One of the introduced diagrammatic approaches is used to recover known results of one-loop renormalization calculations. It is also utilized to calculate the partition function of the $(1+\epsilon)$-state Potts model, and, hence, the generating function for bond percolation, on a finite lattice. This generating function for cluster statistics exhibits the scaling features proposed by Privman and Fisher for systems of finite size.

I. INTRODUCTION

Much is known about percolation and the percolation transition.[1-3] Even so, uncertainties and ambiguities still plague the model on which many of the calculations pertinent to the transition are based. This model was introduced by Fortuin and Kasteleyn,[4] in a seminal paper, in which they established a set of remarkable correspondences between the n-state Potts model[5] in certain limiting regimes and a variety of combinatorial and graph-theoretical problems. In particular, they demonstrated that the derivative with respect to n of the n-state Potts model's partition function in the limit $n=1$ gives rise to the generating function for cluster statistics in bond percolation. Field-theoretical calculations[6-8] of the critical exponents of the percolation transition are carried out on the Ginzburg-Landau-Wilson version of the effective Hamiltonian for the n-state Potts model. In performing the calculations involved, however, one encounters a series of complications.[9] For example, the effective Hamiltonian contains a third-order term, which according to conventional wisdom, dictates a first-order transition to the ordered phase. This prediction of Landau[10] theory is apparently violated in the case of the percolation transition. However, it is violated in the context of the Potts model because one insists, essentially by fiat, that the order parameter take on values that fall within a specified range. The argument in support of this restriction is based on the correspondence between the Potts-model order parameter and a quantity relevant to the percolation transition.[11] While the argument is superficially persuasive, nothing in the steps leading to the effective Hamiltonian lead in a natural way to a restriction on the allowed values of the order parameter.

The perturbation theory of the Potts model at the limit appropriate to percolation contains additional pitfalls. The effective Hamiltonian on which ϵ expansion calculations are based has as its *highest*-order term one that is third order in the order parameter.[12] If one integrates the function $\exp(-ux^3-rx^2)$ over x, the integration contour cannot be taken to $\pm\infty$ on the real axis. It is possible to recover a finite result, but only at the expense of a deformation of the contour that results in a complex value for the integral. In the context of a field-theoretical calculation, a problem analogous to the one above manifests itself in a perturbation series with a "malignant" higher-order limiting form. This issue was addressed by Houghton, Reeve, and Wallace,[9] who carried out an instanton calculation of high-order terms in the perturbation series of the percolation limit of the Potts model. They discovered that it was necessary to reformulate the perturbation-theoretical expansion to recover a series with an asymptotically "benign" form. Their approach is similar to our own. The correspondence between the two methods will be discussed in an appendix.

Both of the issues mentioned above are directly relevant to the problem addressed in this paper—how to arrive at a quantitative description of the percolation transition that yields information in the regime in which finite-size effects are important. We are required to perform an integral over the amplitude of a spatially uniform mode in which we retain the third-order term in the exponent of the Boltzmann factor and must, thus, confront the troubling issues outlined above.

In this paper we report the derivation of an expression for the free energy of the one-state Potts model that yields predictions concerning bond percolation on a finite lattice in the immediate vicinity of the percolation transition. While we are not able to provide a rigorous justification of the expression, we are confident that it is correct in all essentials, and we believe that it can serve as the basis for a comprehensive theoretical investigation of the percolation transition in the finite-size-rounding regime.[13] Furthermore, we are optimistic that in deriving

the expression we have cast a little more light on the kind of extrapolation methods that are utilized in the application of "replication" techniques in statistical mechanics and many-body theory. Thus this work should contribute to progress in understanding the mathematical structure of theoretical models of spin glasses and other random systems.

For future reference, we will, as we have above, refer to the Potts model appropriate to percolation as the one-state Potts model. The actual one-state limit is known to be trivial. As this latter limit also plays a role in the discussion to follow, we will henceforth refer to it as the *strict* one-state Potts model.

An outline of the paper is as follows. In the next section, we introduce the effective Hamiltonian of the n-state Potts model and perform the standard set of transformations and truncations leading to the third-order field theory of the general n-state model. We then formulate the model in such a way as to make it possible to take the $n \rightarrow 1$ limit appropriate to percolation in advance of any other limiting procedures. The results of mean-field theory are recovered. Section III contains a discussion of the renormalization group as it applies to the one-state Potts model. Recursion relations in $6-\epsilon$ dimensions are presented, and the solutions are shown to yield previously calculated exponents. Section IV is devoted to a derivation of the renormalized mean-field theory that constitutes the lowest-order approximation to the behavior of the critical finite system. The ultimate result of this paper is an expression for the free energy of the one-state Potts model in the immediate vicinity of the transition temperature.

II. FORMULATION OF THE PROBLEM

The most straightforward construction of the Ginzburg-Landau-Wilson effective Hamiltonian for the $(1+\epsilon)$-state Potts model utilizes standard arguments based on symmetry. In the case of the n-state Potts mode, the effective Hamiltonian is a functional of an n-component order parameter S_i $(1 \leq i \leq n)$. This functional is invariant under permutation of the components; no other symmetry restricts its form. If we postulate a position-dependent **S** and assume ferromagnetic interactions, we end up with the following expression appropriate to a continuous version of the n-state Potts model:

$$H[\mathbf{S}(\mathbf{x})] = \sum_{i,x} [a_0 S_i(\mathbf{x}) + r S_i(\mathbf{x})^2 + |\nabla S_i(\mathbf{x})|^2 + u S_i(\mathbf{x})^3] \ . \tag{1}$$

Higher-order terms will be less relevant in a renormalization-group sense.

The partition function is the path integral

$$Z = \int \exp\{-H[S(\mathbf{x})]\} \mathcal{D}S(\mathbf{x}) \ . \tag{2}$$

It proves useful to reexpress $\mathbf{S}(\mathbf{x})$ as

$$S_i(\mathbf{x}) = S(\mathbf{x}) + s_i(\mathbf{x}) \ , \tag{3}$$

with the subsidiary condition

$$\sum_i s_i(\mathbf{x}) = 0 \ . \tag{4}$$

The effective Hamiltonian is now given by

$$\begin{aligned} H &= n \left[\sum_{\mathbf{x}} [a_0 S(\mathbf{x}) + r S(\mathbf{x})^2 + |\nabla S(\mathbf{x})|^2 + u S(\mathbf{x})^3] \right] + \sum_{i,x} [r s_i(\mathbf{x})^2 + |\nabla s_i(\mathbf{x})|^2 + u s_i(\mathbf{x})^3] \\ &= n \left[\sum_{\mathbf{x}} [a_0 S(\mathbf{x}) + r S(\mathbf{x})^2 + |\nabla S(\mathbf{x})|^2 + u S(\mathbf{x})^3] \right] + H[s_i(\mathbf{x})] \ . \end{aligned} \tag{5}$$

We ignore the first line on the right-hand side of Eq. (5), because we anticipate that the integration over $S(\mathbf{x})$ will yield an uninteresting contribution to the partition function. The percolation transition arises from the integration over the s_i's.

The partition function in the limit $n=1$ is trivial in that the only way to satisfy the constraint equation (4) is to set the single component of the one-dimensional vector $\mathbf{s}(\mathbf{x})$ equal to zero. However, as noted in the Introduction, the quantity of interest is the *derivative* of the partition function with respect to n at $n=1$. Two methods of evaluating the appropriate limiting form of the partition function have been described in the literature.[6,9] In the first method, one replaces the s_i's by the diagonal entries of a traceless, symmetric $n \times n$ matrix.[6] The first ϵ-expansion calculations were performed with the use of this approach. The second procedure was developed to produce a benign form for the high-order terms in a perturbation expansion (in powers of u) of the $(1+\epsilon)$-state Potts-model partition function.[9] This latter approach is based on the introduction of a ghost field into the Hamiltonian. The s_i's are no longer subject to the constraint equation (4). In the work reported here, we utilize a third method, to be described immediately below. As is shown in Appendix A, this method is equivalent to both of the approaches above. It also leads to yet *another* variation of perturbation theory for the $(1+\epsilon)$-state Potts model. This fourth technique is also described in Appendix A.

The key step in evaluating the partition function is to replace the site-by-site constraint (4) with its representation as a Fourier functional integral:

$$\delta \left[\sum_i s_i(\mathbf{x}) \right] = \frac{1}{2\pi} \int \exp \left[i\omega(\mathbf{x}) \sum_i s_i(\mathbf{x}) \right] d\omega(\mathbf{x}) \ . \tag{6}$$

We thus introduce a new field $\omega(\mathbf{x})$, conjugate to $\sum_i s_i(\mathbf{x})$. This method is strongly reminiscent of a key element of the Martin-Siggia-Rose development of perturbation theory for semimicroscopic dynamical systems[14] and to

the Fadeev-Popov method of gauge fixing.[15]

The immediate effect of this representation of the δ function is that, prior to the integration over the field $\omega(\mathbf{x})$, the $s_i(\mathbf{x})$'s are decoupled in the effective Hamiltonian. We have, when $n=1+\epsilon$,

$$Z_n=\int \exp\left[\sum_{i,x} -[rs_i(\mathbf{x})^2+|\nabla s_i(\mathbf{x})|^2+us_i(\mathbf{x})^3 +i\omega(\mathbf{x})s_i(\mathbf{x})]\right]\mathcal{D}\omega(\mathbf{x})\mathcal{D}s_i(\mathbf{x}) =\int \{Z[\omega(\mathbf{x})]\}^{1+\epsilon}\mathcal{D}\omega(\mathbf{x})$$

and, thus,

$$Z_n\to\int \{Z[\omega(\mathbf{x})]\}(1+\epsilon\ln\{Z[\omega(\mathbf{x})]\}+\cdots)\mathcal{D}\omega(\mathbf{x})\ . \tag{7}$$

The quantity of interest is thus

$$\frac{Z_{1+\epsilon}-Z_1}{\epsilon}=\int Z[\omega(\mathbf{x})]\ln\{Z[\omega(\mathbf{x})]\}\mathcal{D}(\omega(\mathbf{x}))\ . \tag{8}$$

It is worth noting that we have taken the limit applicable to percolation prior to taking any other limits—in particular the thermodynamic limit. This is the basis of our claim that the procedure readily lends itself to finite-size analysis. An important feature of the effective Hamiltonian in Eqs. (6)–(8) requires our attention. Because the highest-order term in it is third order, the nominal integration contour for $s_i(\mathbf{x})$ along the real axis is not proper in a formal sense, in that, as $s_i(\mathbf{x})$ becomes large and negative, the Boltzmann factor $\exp(-H)$ grows without bound. As a result, the partition-function integral will diverge. A possible remedy is to deform the contour so as to ensure the integral's convergence. The price that is exacted for this cure is the possibility of an imaginary contribution to the partition function. Results that we believe to be correct are obtained if one takes as the partition function the *real* part of the integral with the deformed contour. We have no proof that this is the proper prescription, but we will present evidence that we consider to be highly persuasive.

One is led to consider the one-dimensional integral

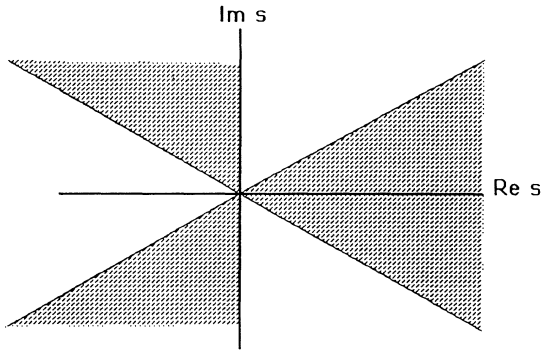

FIG. 1. Regions, shown shaded, in which the integration contour must lie, for asymptotically large magnitudes of $|s|$, in order that the integral on the right-hand side of Eq. (9) converges.

$$I(r,u,\omega)=\int \exp(-us^3-rs+i\omega s)ds\ . \tag{9}$$

Convergent contours for this integral must lie, for asymptotically large $|s|$, in the shaded regions in Fig. 1.

A few straightforward changes of variables transform the integral in Eq. (9) to

$$\exp\left[-\frac{2r^3}{27u^2}-\frac{i\omega r}{3u}\right]\int \exp\left[-us^3+\left[i\omega+\frac{r^2}{3u}\right]s\right]ds\ . \tag{10}$$

Now we take as the contour of integration for s the downward sloping line making an angle of $\pi/6$ with the real axis. The integral in Eq. (10) becomes

$$\int \exp\left[ius^3+\left[i\omega+\frac{r^2}{3u}\right]e^{-i\pi/6}s\right]e^{-i\pi/6}ds\ . \tag{11}$$

At the same time, we require that integrations over ω be along the *upward* sloping line making an angle of $\pi/6$ with respect to the real ω axis. This is tantamount to replacing ω by $\omega e^{i\pi/6}$ and $d\omega$ by $d\omega e^{i\pi/6}$. Neglecting factors associated with ds and the yet-to-be-introduced $d\omega$, we are left with

$$I(r,u,\omega)=\exp\left[-\frac{2r^3}{27u^2}+\frac{\omega r}{3u}e^{-i\pi/3}\right](3u)^{-1/3}\int_{-\infty}^{\infty}\exp\left[ius^3+\left[i\omega+\frac{r^2}{3u}e^{-i\pi/6}\right]s\right]ds$$
$$=\exp\left[-\frac{2r^3}{27u^2}+\frac{\omega r}{3u}e^{-i\pi/3}\right](3u)^{-1/3}\mathrm{Ai}\left[\frac{1}{(3u)^{1/3}}\left[\omega+\frac{r^2}{3u}e^{-2\pi i/3}\right]\right]\ . \tag{12}$$

In the last line of Eq. (12), the function Ai is one of the Airy functions.[16] The result embodied in Eq. (12) plays an important role in the evaluation of the integral in Eq. (8) and in the evaluation of the mean-field partition function.

A. Mean-field theory

The approximation leading to mean-field theory replaces the spatially fluctuating $s_i(\mathbf{x})$'s by uniform fields s_i. The integrals to be performed are those discussed im-

mediately above, except that the coefficients r and u and the variable ω are multiplied by the factor N, where N is the number of lattice sites in the system. The mean-field partition function is

$$\int I(Nr,Nu,N\omega)\ln[e^{-i\pi/6}I(Nr,Nu,N\omega)]d(N\omega)\ . \quad (13)$$

To proceed with the evaluation of the integral, we note that $I(Nr,Nu,N\omega)$, as a function of ω, has no singularities anywhere in the complex ω plane, as long as ω is finite. The logarithmic term will have branch points wherever the function $I(Nr,Nu,N\omega)$ passes through zero. Because of the relation of I to the Airy function, we know that these zeros are confined to a line parallel to the real ω axis with one end at $\omega=r^2e^{i\pi/3}/3u$ and extending out to $\omega=-\infty$. These branch points are the only nonanalyticities of $\ln(I)$ in the vicinity of the real ω axis. We can thus replace the logarithm in the integral by

$$\frac{1}{2\pi}\int_C \frac{F(\omega')}{\omega-\omega'}d\omega' , \quad (14)$$

where $F(\omega)=\ln(I)$ and the contour is as indicated in Fig. 2.

Now, if the contour is sufficiently far above or below the real ω axis, we can replace the function I by

$$\int_{-\infty}^{\infty} e^{Ni\omega s}ds=\delta(N\omega) , \quad (15)$$

and the result of the integration over $N\omega$ is

$$Z=\int \frac{F(\omega')}{-\omega'}d\omega'=\ln[e^{-i\pi/6}I(Nr,Nu,0)] . \quad (16)$$

This result for $\ln(Z)$ also follows directly from Eq. (13) if one uses a Mittag-Lefler expansion of $I'(\omega)/I(\omega)$, as long as the temperature is not too close to the transition temperature or, in the case of percolation, as long as the probability of a bond being active is not too close to the critical value. We now utilize Eq. (12) and the asymptotic form of the Airy function[16]

$$\mathrm{Ai}(\omega)\rightarrow\zeta^{-1/4}e^{-\zeta^{3/2}} , \quad (17)$$

where $\zeta=\frac{2}{3}\omega^{2/3}$. The above asymptotic form of the Airy function is valid when $|\omega|$ is large and ω is not on the negative real axis. We obtain

$$Z\rightarrow N\left[\frac{-2r^3}{27u^2}+\frac{2|r|^3}{27u^2}\right]+O(1) . \quad (18)$$

The expression above has precisely the behavior one expects for the Ginzburg-Landau theory of the percolation transition. An important feature of Eq. (18) is that the $O(1)$ term contains *no* imaginary contributions. The factor $e^{-i\pi/6}$ is canceled by a compensating complex exponential in the term $\zeta^{-1/4}$.

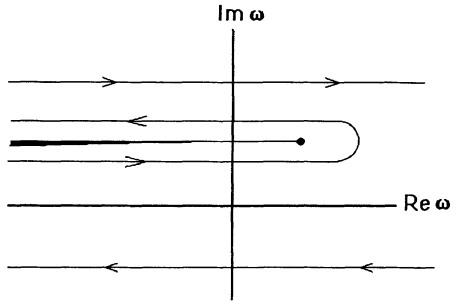

FIG. 2. Contour of integration for the integral in Eq. (14).

The expression above holds as long as the system is not so close to the bulk transition that finite-size effects come into play. It is possible to extract the leading-order corrections to Eq. (18) in the bulk critical region. They are of the form u^2/Nr^3. This last result provides a measure, in the context of mean-field theory, of size of the region within which finite-size effects play an important role. There is a dimensionality in which the criterion $r^3\sim u^2/N$ is consistent with the both mean-field theory and the standard finite-size scaling hypothesis for the crossover to finite-size-effect dominance,[17] specifically, there is crossover to finite-size behavior when $\xi\sim L$, where ξ, the correlation length, is proportional to $(T-T_0)^{-\nu}$ and L is the linear dimension of the finite system. Setting $\nu=\frac{1}{2}$ we find that the special dimensionality of the system is 6, the *upper critical dimensionality* of the percolation system. If a renormalized mean-field theory is possible, the criterion above ought to be adaptable to accommodate nonclassical exponents and a variety of spatial dimensionalities, in particular to $6-\epsilon$ dimensions.

As mentioned previously, demanding that the integrals over ω converge requires that the partition function be defined as the real part of the integral given in expression (13). There is an independent way to demonstrate the correctness of this prescription; Eq. (13) can be manipulated to yield an expression that corresponds to a limiting result derived by two of us in an analysis of the infinite range and, hence, the mean-field one-state Potts model.[11] The steps taken in this previous work are not related in any obvious way to those described above, and the partition function derived by Rudnick and Gaspari is unquestionably real.

B. Correspondence with earlier work

Consider the mean-field partition function as defined by (13), with the requirement of reality explicitly incorporated:

$$Z=\mathrm{Re}\left\{\int d\omega\left[\int \exp(Nius^3-Nrs^2e^{-2\pi i/3}+iN\omega s)ds\ \ln[I(Nr,Nu,N\omega)]\right]\right\} . \quad (19)$$

Given that the singularities of $\ln[I]$ as a function of ω are all in the upper half of the complex plane, we can restrict the integral over s in Eq. (19) to $s>0$. Now alter the contours of integration over s and ω by shifting them back to their original orientations in the complex planes, i.e.,

$$s \rightarrow s \exp(i\pi/6), \quad \omega \rightarrow \omega \exp[-i\pi/6)] .$$

Then

$$Z = \mathrm{Re}\left\{ \int d\omega \left[\int \exp(-Nus^3 - Nrs^2 + iN\omega s) ds \ln[I(Nr, Nu, N\omega\epsilon^{-i\pi/6})] \right] \right\} . \tag{20}$$

Finally, we rotate the ω-integration contour to the imaginary axis. This yields

$$\begin{aligned} Z &= \mathrm{Re}\left\{ \int -i\, d\Omega \left[\int \exp(-Nus^3 - Nrs^2 + N\Omega s) ds \ln[I(Nr, Nu, -iN\Omega e^{-i\pi/6})] \right] \right\} \\ &= \mathrm{Im}\left\{ \int d\Omega \left[\int \exp(-Nus^3 - Nrs^2 + N\Omega s + N\Omega s) ds \ln[I(Nr, Nu, N\Omega\epsilon^{-2\pi i/3})] \right] \right\} . \end{aligned} \tag{21}$$

The function $I[Nr, Nu, N\omega e^{-2\pi i/3}]$ is equal to the integral

$$\int ds' \exp(-Nus'^3 - Nrs'^2 + N\Omega s') , \tag{22}$$

where $s' = s'' e^{-i\pi/6}$. If we shift s' so as to eliminate the quadratic term in the exponential, making the replacement

$$s' \rightarrow s' - \frac{r}{3u} , \tag{23}$$

we have

$$us'^3 + rs'^2 - \Omega s' \rightarrow us'^3 + \frac{s'r^2}{3u} - \frac{2r^3}{27u^2} - \Omega s' + \frac{\Omega r}{3u} . \tag{24}$$

Now let $\Omega \rightarrow \Omega + r^2/3u$. The exponent in Eq. (22) becomes

$$us'^3 + \frac{r^3}{27u^3} - \Omega s' \tag{25}$$

and

$$I \rightarrow \int ds' \exp[-N(us'^3 - \Omega s')] \exp\left[-\frac{Nr^3}{27u^2} - \frac{N\Omega r}{3u} \right] . \tag{26}$$

Because we are interested in the imaginary part of the logarithm of I, the exponential multiplying the integral can be discarded. The partition function is now given by

$$Z = \int_{-\infty}^{\infty} d\Omega \int_0^{\infty} ds \exp\left\{ N\left[-u\left[s + \frac{r}{3u} \right]^3 + \frac{r^3}{27u^2} + \Omega s \right] \right\} \mathrm{Im}\left[\ln\left[\int ds' \exp(-N[us'^3 - \Omega s']) \right] \right] , \tag{27}$$

where the shift in Ω has been taken into account in the integral over the variable s. Once appropriate correspondence have been made, this result is essentially identical to Eq. (49) in Ref. 11, which is an expression for the partition function of the strict mean-field one-state Potts model in the immediate vicinity of the transition temperature.

It is clear that a good deal of necessary discussion has been left out of the derivation of Eq. (27). Needless to say, we believe that a proper consideration of issues relating to the convergence of integrals and the freedom to close contours at infinity will yield a full justification of the above form for Z. However, the fact that it matches previously derived results provides a persuasive, if not absolutely compelling, argument for its correctness.

III. RENORMALIZATION GROUP

The key to the calculation of renormalized quantities is an identity that holds between two types of propagators. The first is the ϕ-connected contribution to $\langle s(\mathbf{x}_1) s(\mathbf{x}_2) \rangle$. (Note that we use the phrase "ϕ-connected" even though it is inconsistent with our notation to maintain consistency with the terminology of Houghton, Reeve, and Wallace[9] whose method is close in spirit to the method used here.) This propagator is the sum of contributions of the diagrammatic form illustrated in Fig. 3. Appendix A contains an explanation of the diagrams. The diagrams shown in Fig. 3 have the property that they remain connected when lines with an x in them are cut. The exception to the above rule is exemplified by the last diagram in the figure, in which cutting all "x propagators" liberates *isolated* (i.e., unrenormalized) three-point vertices. These isolated vertices will play an important role in the analysis that follows. They represent the lowest-order unrenormalized contribution to a class of three-point vertices denoted by the symbol v_C (represented graphically as shown in Fig. 5). At lowest order the "disconnected" vertex v_C is equal and opposite in strength to the unrenormalized "connected" three-point

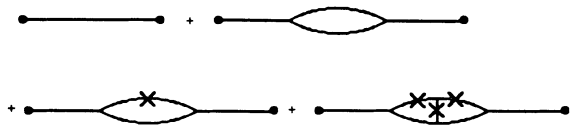

FIG. 3. Contributions to the f-connected propagator.

vertex v_A (also depicted in Fig. 5).

The second type of propagator is ϕ *disconnected.* A few contributions to this propagator are displayed in Fig. 4. These propagators fall into exactly two pieces, each containing one of the two terminal dots, when "x propagators" are cut. As in the previous case, there is an exception in that isolated three-point vertices may also be liberated as a result of the process of severing x propagators.

If we denote by $G_c(\mathbf{x}_1,\mathbf{x}_2)$ the sum of all contributions to ϕ-connected propagators and let $G_d(\mathbf{x}_1,\mathbf{x}_2)$ stand for all contributions to ϕ-disconnected propagators, the identity referred to above is

$$G_c(\mathbf{x}_1,\mathbf{x}_2)+G_d(\mathbf{x}_1,\mathbf{x}_2)=0 \ . \tag{28}$$

This identity follows from

$$\begin{aligned}\int s(\mathbf{x}_1)s(\mathbf{x}_2)\exp\left[-H[s(\mathbf{x})]+i\sum_{\mathbf{x}}\omega(\mathbf{x})s(\mathbf{x})\right]&\mathcal{D}_S(\mathbf{x})\mathcal{D}(\mathbf{x})\\ &=G_c(\mathbf{x}_1,\mathbf{x}_2)+G_d(\mathbf{x}_1,\mathbf{x}_2)\\ &=\int s(\mathbf{x}_1)s(\mathbf{x}_2)\exp\{-H[s(\mathbf{x})]\}\prod_i\delta(s(\mathbf{x}_i))\mathcal{D}_S(\mathbf{x})\\ &=0 \ .\end{aligned} \tag{29}$$

The second line in Eq. (29) follows from a consideration of the diagrams generated when one integrates over $s(\mathbf{x})$ and then over $\omega(\mathbf{x})$. Once again, the reader is referred to Appendix B. The equality on the third line is obtained by integrating over $\omega(\mathbf{x})$. The fourth line follows immediately.

The renormalization of vertices proceeds straightforwardly. For example, we may consider the lowest-order contributions to the renormalization of a ϕ-connected three-point vertex, displayed in Fig. 11. Because of the relation above, which holds *whether the propagator lines are renormalized or not,* we have for this contribution the net combinatorial factor of -2 $(+1$ from the first diagram and -3 from the second one). In order to fully evaluate vertex renormalization, it is necessary to define three types of vertices. They are (1) a vertex in which ϕ connects all three of the lines that attach to it, which we call v_A, (2) a vertex which ϕ connects only two of them, v_B, and (3) a vertex in which all three lines are ϕ disconnected, v_C. The graphical representation of those vertices and one-loop contributions to them are displayed in Fig. 5. An important rule in the diagrammatic construction of the vertices and in the construction of all quantities of interest here is that there may be no ϕ-disconnected internal portions. Utilizing the three vertices above, we can construct the one-loop contributions to the renormalization of each of them.

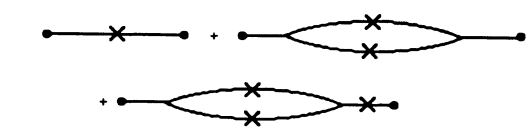

FIG. 4. Contributions to the f-disconnected propagator.

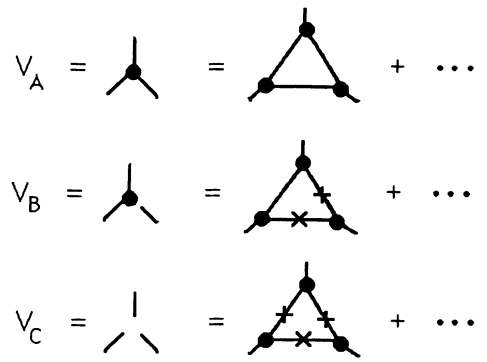

FIG. 5. Diagrammatic representations and low-order contributions to the three vertices defined above.

As it turns out, we do not need to analyze the full set of equations. This is because they are all consistent with the relations $v_A=-v_C$ and $v_B=0$. Furthermore, as noted above, these relations are satisfied as initial conditions. The one-loop renormalization-group recursion relations in $6-\epsilon$ dimension are

$$\begin{aligned}\frac{dv_A}{dl}&=\left[d-\frac{3}{2}(d-2+\eta)\right]v_A-72A_6v_A^3\\ &=\frac{\epsilon}{2}V_A-\frac{3}{2}\eta v_A-72A_6v_A^3 \ ,\end{aligned} \tag{30}$$

$$\eta=-6A_6v_A^2 \ , \tag{31}$$

$$v_C=-v_A \ , \tag{32}$$

$$v_B=0 \ . \tag{33}$$

For a discussion of the diagrams contributing to the equations above, see Appendix B.

The stable fixed point solution of Eq. (30) is

$$v_A^2=\frac{\epsilon}{126A_6} \ . \tag{34}$$

This and Eq. (31) imply

$$\eta=-\frac{\epsilon}{21} \ . \tag{35}$$

The critical exponent $y=1/\nu$ is obtained by solving for the exponential growth of r, the renormalized reduced temperature, where r satisfies the equation

$$\begin{aligned}\frac{dr}{dt}&=(2-\eta)r-36A_6v_A^2r\\ &=(2-\tfrac{5}{21}\epsilon)r\\ &\equiv yr \ .\end{aligned}$$

These results for y and η are entirely consistent with the ϵ expansions previously obtained with the use of traceless symmetric tensors.[6,7]

IV. RENORMALIZED MEAN-FIELD THEORY

Because of the way in which diagrams are generated, it is not immediately obvious that fluctuations act to renormalize mean-field theory as one might *a priori* expect. According to such expectations, the lowest-order-in-ϵ version of the finite-system partition function is just the right-hand side of Eq. (13) [or Eq. (27)], with the parameters r, u, ω (or Ω), and s suitably renormalized and rescaled.[18] However, we know that there can be *no* fluctuation corrections to the exponent in Eq. (13), because the integration over ω leads to a cancellation of all terms arising from the functional integral over s, unless there is a "coupling" with diagrams from within the logarithm. As it turns out, mean-field theory is, indeed, renormalized in the expected manner, but the perturbation-theoretical demonstration is not entirely direct. It relies on the identity relating renormalized three-point vertices that played a key simplifying role in the derivation of the renormalization-group results of the previous subsection.

We start with the Feynman-graph expansion for the one-state Potts-model partition function. Now we distinguish between propagator lines for the $\mathbf{q}=0$, or uniform, modes and those for all the other $s(\mathbf{q})$'s. We organize the diagrams according to loop order with respect to the $\mathbf{q}=0$ propagator lines. At lowest nontrivial order, the diagrams contributing to the partition function are as shown in Fig. 6(a). The vertices and propagators in Fig. 6 are taken to be fully renormalized with respect to all $\mathbf{q}\neq 0$ fluctuations. Note that all diagrams are ϕ connected in the sense established in Sec. III. The bottom vertex in the diagram on the left in Fig. 6(a), in which all the external legs are ϕ disconnected, was denoted by v_C earlier. All other vertices, which "ϕ-connect" external legs, are of the type v_A. Now, as established to lowest order, the $\epsilon=6-d$ expansion, $v_C=-v_A$. Furthermore, $v_B=0$. Thus there is no contribution to the partition function from the diagram displayed in Fig. 6(b).

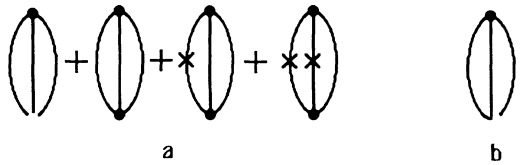

FIG. 6. (a) Diagrams contributing to the two-loop-order renormalized mean-field-theory free energy. (b) A diagram that does not contribute to the free energy, because the vertex at the bottom of the diagram is equal to zero.

We now appeal to the identity, expressed in Eq. (28), between ϕ-connected and ϕ-disconnected propagators to establish the equality displayed in Fig. 7(a), which implies that the diagram sum in Fig. 7(b) is equal to the lowest-nontrivial-order loop contribution to the renormalized partition function. This digram sum is *precisely* what one obtains from Eq. (13) with parameters r and u replaced by their renormalized counterparts. An extension of the demonstration to higher-order diagrams is straightforward to construct.

Note that our argument rests on a relation between three-point vertices that we have shown to hold up to one-loop order. Although we have not demonstrated that this identity holds in general, we are confident that it does and that it is based on a relationship such as the one leading to the identity (23) between G_c and $-G_d$.

Putting together all the preceding elements, we arrive at a simple expression for the partition function of the finite one-state Potts-model system:

$$Z=\int_{-\infty}^{\infty} d\Omega \int_0^{\infty} ds \exp\left[-u^*\left[s+\frac{tL^{1/\nu}}{3u^*}\right]^3+\frac{(tL^{1/\nu})^3}{27u^{*2}}+\Omega s\right] \mathrm{Im}\left[\ln\left[\int ds' \exp-(u^* s'^3-\Omega s')\right]\right] . \tag{36}$$

This result holds in the immediate vicinity of the bulk critical point under the assumption that the bulk correlation length is much larger than a characteristic linear dimension L of the system ($t^{-\nu}\gg L$). The system is confined to a d-dimensional hypercubic volume with length per side equal to L. In Eq. (36) the quantity u^* is the fixed-point value of the third-order coupling and t is the reduced temperature [$t\propto(T-T_c)/T_c$]. Setting $t=0$, we immediately obtain from Eq. (36) an expression from which we can extract a universal value for the finite-system partition function (or the percolating-system-generating function) at the bulk transition point, in accord with the Privman-Fisher hypothesis.[19,20]

Thus we see that the renormalized partition function, when evaluated beyond steepest descents, yields a description of the percolation transition on a lattice of finite size. We expect a rounding of singularities and appropriate corrections to bulk-limit results. While there are still loose ends, we feel that a start has been made and that there is a basis for significant future progress. It will be interesting to compare predictions based on Eq. (36) with the results of simulations. Such a comparison will be the subject of future work.

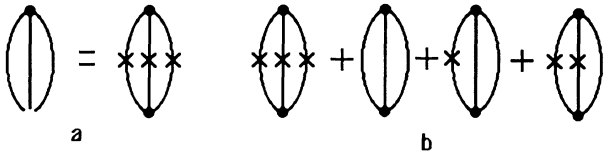

FIG. 7. (a) Diagrammatic identity leading to the result that the two-loop renormalized partition function is given by the diagram sum displayed in (b).

APPENDIX A: EQUIVALENCE OF THE VARIOUS APPROACHES TO PERTURBATION THEORY OF THE ONE-STATE POTTS MODEL

1. Traditional approach (Refs. 6 and 7)

Here the constraint (4) on the s_i's is satisfied by writing

$$s_n = -s_1 - s_2 - \cdots - s_{n-1} . \tag{A1}$$

The quadratic term in the effective Hamiltonian is of the form

$$\alpha(s_1^2 + \cdots + s_{n-1}^2) + \alpha(-s_1 - \cdots - s_{n-1})^2 , \tag{A2}$$

where the position or wave-vector dependence of all terms has been suppressed. If we regard the s_i's $(1 \le i \le n-1)$ as the component of an $(n-1)$-dimensional vector, then the quadratic coefficient can be represented in tensor notation as

$$\alpha(\mathbb{1} + |\psi\rangle\langle\psi|) , \tag{A3}$$

where $\mathbb{1}$ is the $(n-1)\times(n-1)$ identity matrix and $|\psi\rangle$ is the column vector

$$|\psi\rangle = \begin{pmatrix} s_1 \\ s_2 \\ \cdot \\ \cdot \\ \cdot \\ s_{n-1} \end{pmatrix} . \tag{A4}$$

The propagator in perturbation theory, which is the inverse of (A3), will then be

$$G = \frac{1}{\alpha}\left[\mathbb{1} - \frac{1}{n}|\psi\rangle\langle\psi|\right] . \tag{A5}$$

The diagonal elements of this $(n-1)\times(n-1)$ matrix are

$$\langle s_i|G|s_j\rangle = \frac{1}{\alpha}\left[\delta_{ij} - \frac{1}{n}\right] . \tag{A6}$$

Furthermore,

$$\langle\psi|G|s_i\rangle = \langle s_i|G|\psi\rangle = -\frac{1}{n\alpha} \tag{A7}$$

and

$$\langle\psi|G|\psi\rangle = \frac{1}{\alpha}\left[1 - \frac{1}{n}\right] . \tag{A8}$$

The above relationships imply

$$G_{ij} = \langle s_i|G|s_j\rangle = \frac{1}{\alpha}\left[\delta_{ij} - \frac{1}{n}\right] \tag{A9}$$

for *all* i and j, including i and/or $j = n$. Now the diagrams in the perturbation expansion consists of third-order vertices arising from the terms vs_i^3 that are connected by propagator lines of the form G_{ij} as given by (A9). This is the perturbation expansion utilized by Priest and Lubensky.[7]

2. Present method

Here the Fourier representation (6) of the δ function that enforces the constraint (4) introduces linear terms into the effective Hamiltonians of the individual s_i's. If, prior to the integrations over the $\omega(\mathbf{x})$'s, the $s_i(\mathbf{x})$'s are integrated out, one obtains a Feynman-diagrammatic expansion containing terms like those shown in Fig. 8. The x's at the ends of the dangling lines stand for factor of $i\omega(\mathbf{x})$. The single lines are unrenormalized propagators $G(\mathbf{x},\mathbf{x}')$, where

$$G^{-1}(\mathbf{x},\mathbf{x}') = \tfrac{1}{2}[r\delta(\mathbf{x}-\mathbf{x}') + \delta''(\mathbf{x}-\mathbf{x}')] ; \tag{A10}$$

i.e., the first diagram above stands for

$$\sum_{\mathbf{x},\mathbf{x}'} i\omega(\mathbf{x})G(\mathbf{x},\mathbf{x}')i\omega(\mathbf{x}') . \tag{A11}$$

The subsequent integrations over the $\omega(\mathbf{x})$'s result in contractions of the lines. This is achieved by expanding the exponential consisting of all connected diagrams with respect to all diagrams *except* the diagram representing (A11). The result of the final set of integrations and reexponentiations is a set of diagrams containing two kinds of unrenormalized propagator. The first is a solid line, representing the propagator generated as a result of the integration over the $s(\mathbf{x})$'s. The second, a solid line with a cross in the middle, is the result of the contraction of two lines each ending in a cross. An example of a low-order diagram generated by this procedure is displayed in Fig. 9. The two upper propagators on the top of that diagram, which we call x propagators, are the result of the contraction of two propagators ending in $i\omega(\mathbf{x})$'s. Each of these propagators is of the form

$$\begin{aligned} G_d(\mathbf{x},\mathbf{x}') &= -\sum_{\mathbf{x}_1,\mathbf{x}_2} G(\mathbf{x},\mathbf{x}_1)G^{-1}(\mathbf{x}_1,\mathbf{x}_2)G(\mathbf{x}_2,\mathbf{x}') \\ &= -G(\mathbf{x},\mathbf{x}') . \end{aligned} \tag{A12}$$

The relation above—between propagators that fall into two pieces when lines are cut at x's, i.e., x propagators and those that do not hold—holds at all orders in perturbation theory. A demonstration of this can be found in Sec. III.

3. Ghost-field method of Houghton, Reeve, and Wallace

In order to derive the formulation of Houghton, Reeve, and Wallace, we rewrite the effective Hamiltonian in

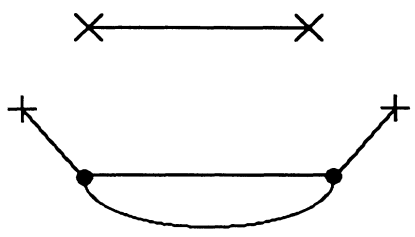

FIG. 8. Diagrams generated by the integration over the $si(\mathbf{x})$'s. The crosses stand for factors of $i\omega(\mathbf{x})$.

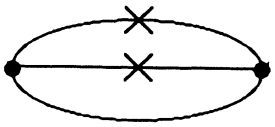

FIG. 9. Low-order diagram resulting from integration over the $s(\mathbf{x})$'s and the $\omega(\mathbf{x})$'s.

terms of the spatial Fourier transform of the order-parameter field. For the time being, we only need to display the quadratic terms in the effective Hamiltonian:

$$H_2[\mathbf{s}(\mathbf{q})]=\sum_{\mathbf{q},i}[s_i(\mathbf{q})s_i(-\mathbf{q})(r+A|\mathbf{q}|^2) +i\omega(\mathbf{q})s_i(-\mathbf{q})] \equiv\sum_{\mathbf{q},i}[\alpha(\mathbf{q})s_i(\mathbf{q})s_i(-\mathbf{q})+i\omega(\mathbf{q})s_i(-\mathbf{q})] . \quad \text{(A13)}$$

As before, integration over $\omega(\mathbf{q})$ enforces the constraint on the sum of the s_i's. Now redefine $\omega(\mathbf{q})$ as

$$\omega(\mathbf{q})\equiv 2\alpha(\mathbf{q})\Omega(\mathbf{q}) . \quad \text{(A14)}$$

The quadratic terms are now, for fixed $\mathbf{q}$,

$$\alpha(\mathbf{q})\sum_i s_i(\mathbf{q})s_i(-\mathbf{q})+2i\alpha(\mathbf{q})\Omega(\mathbf{q})\sum_i s_i(-\mathbf{q}) . \quad \text{(A15)}$$

We now redefine $\Omega(\mathbf{q})$ as the ghost field $s_g(\mathbf{q})$. If we shift $s_i(\mathbf{q})$ by $-is_g(\mathbf{q})$, the effective Hamiltonian takes the form

$$\alpha(\mathbf{q})\sum_i[s_i(\mathbf{q})-is_g(\mathbf{q})]^2-2i\alpha(\mathbf{q})s_g(\mathbf{q})\sum_i s_i(\mathbf{q}) =\alpha(\mathbf{q})\sum_i s_i(\mathbf{q})s_i(-\mathbf{q})+n\alpha(\mathbf{q})s_g(\mathbf{q})s_g(-\mathbf{q}) . \quad \text{(A16)}$$

Our functional integral is over n fields S_i and an additional ghost field s_g. The third-order term in the effective Hamiltonian is of the form $\sum_i(s_1-is_g)^3$. If we let $s_g\rightarrow is_g$, then we recover the effective Hamiltonian of Houghton, Reeve, and Wallace. The propagator for s_g is equal and opposite to the propagator for s_i, and there is a natural cancellation of all diagrams that are not ϕ connected.

4. Fourth perturbation-theoretical approach

The exponent in the function whose integration yields the partition functional Z, as defined in Eq. (7), has the general form

$$-H[s(\mathbf{q})]=-\{f[s(\mathbf{q})]-i\omega(\mathbf{q})s(-\mathbf{q})\} , \quad \text{(A17)}$$

if we replace the order-parameter field by its spatial Fourier transform. Sums over $\mathbf{q}$ are understood. Now we write

$$f[s(\mathbf{q})]=\tfrac{1}{2}f''s(\mathbf{q})s(-\mathbf{q})+F[s(\mathbf{q})] , \quad \text{(A18)}$$

where the functional F consists of third- and higher-order terms. We rewrite $\omega(\mathbf{q})$ as $f''\omega(\mathbf{q})$. The linear and quadratic terms in the effective Hamiltonian then take the form

$$\tfrac{1}{2}f''[s(\mathbf{q})-i\omega(\mathbf{q})][s(-\mathbf{q})-\omega(-\mathbf{q})]+\tfrac{1}{2}f''\omega(\mathbf{q})\omega(-\mathbf{q}) . \quad \text{(A19)}$$

If we redefine $s(\mathbf{q})$ as $s(\mathbf{q})-i\omega(\mathbf{q})$, the exponent takes the form

$$H'[s(\mathbf{q})]=\tfrac{1}{2}f''[s(\mathbf{q})s(-\mathbf{q})+\omega(\mathbf{q})\omega(-\mathbf{q})] +F[s(\mathbf{q})+i\omega(\mathbf{q})] . \quad \text{(A20)}$$

Now, defining

$$s_\pm(\mathbf{q})\equiv s(\mathbf{q})\pm i\omega(\mathbf{q}) , \quad \text{(A21)}$$

the right-hand side of (A20) has the form

$$h[s_+(\mathbf{q}),s_-(\mathbf{q})]=\tfrac{1}{2}f''s_+(\mathbf{q})s_-(-\mathbf{q})-F[s_+(\mathbf{q})] . \quad \text{(A22)}$$

The rules for forming Feynman diagrams are that all third- and higher-order vertices have lines *emerging* from them, as displayed in Fig. 10(a). These lines are associated with factors of s_+. Pairings are allowed only between an s_+ and an s_-. It is an essentially trivial exercise to verify that the integral

$$\int\exp\{h[s_+(\mathbf{q}),s_-(\mathbf{q})]\}\mathcal{D}s_+(\mathbf{q})\mathcal{D}s_-(\mathbf{q})$$

contains no contribution from the third- and higher-order interactions. However, to calculate the percolation-generating function, we must multiply the partition functional Z by the logarithm of another integral. Using the reparametrizations above, the integrand is

$$\exp\{-\tfrac{1}{2}f''s(\mathbf{q})s(-\mathbf{q})-F[s(\mathbf{q})] +\tfrac{1}{2}[s_+(\mathbf{q})-s_-(\mathbf{q})]s(-\mathbf{q})\} . \quad \text{(A23)}$$

The functional integral over $s(\mathbf{q})$ yields connected diagrams having dangling lines that both *emerge* from vertices, corresponding to factors of $s_+(\mathbf{q})$, and that *point into* them, corresponding to factors of $s_-(\mathbf{q})$. An example is displayed in Fig. 10(b). The subsequent integrations over $s_+(\mathbf{q})$ and $s_-(\mathbf{q})$ give rise to nontrivial corrections to the bare theory. The explicit notion of ϕ connectedness does not enter.

From this point on, it is straightforward to derive the rules for Feynman diagrams. As we do not make use of this approach in the work reported here, we leave further development to the reader.

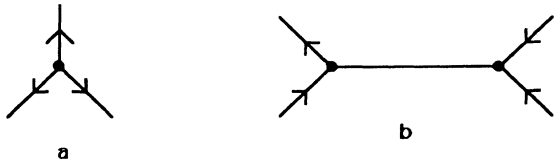

FIG. 10. Diagrams appearing in (a) the partition function Z and (b) the logarithmic factor multiplying Z in the calculation of the percolation-generating function.

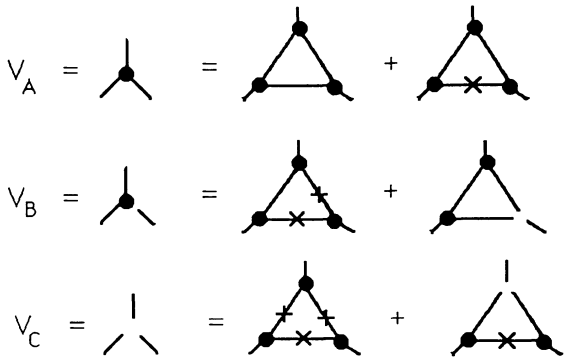

FIG. 11. One-loop diagrammatic contributions to the three three-point vertices v_A, v_B, and v_C.

APPENDIX B: RENORMALIZATION-GROUP CALCULATIONS

Under the assumption that the relations $v_A = -v_C$ and $v_B = 0$ hold between the vertices defined in Fig. 5, the one-loop contributions to the three vertices are summarized in Fig. 11. After a straightforward calculation, we find that the two diagrams contributing to v_B cancel and that the relation $v_A = -v_C$ is preserved. In order to construct the full one-loop renormalization-group recursion relations for the three-point vertices, it is necessary to calculate the anomalous dimension η to one-loop order. The diagrams contributing to η at one-loop order are shown in Fig. 12. The requisite angular integrations have been discussed in the literature.[7] If we define A_6 as the result of an integration over the surface of a six-dimensional sphere with unit radius, we obtain Eqs. (30)–(33).

FIG. 12. Two diagrams contributing to the mass operator and, hence, to the critical exponent h at one-loop order.

*Present address: Department of Physics, Case Western Reserve University, 10900 Euclid Ave., Cleveland, Ohio 44106.

[1]S. R. Broadbent and J. M. Hammersly, Proc. Cambridge Philos. Soc. **53**, 629 (1957).
[2]H. L. Frisch and J. M. Hammersly, J. Soc. Ind. Appl. Math. **11**, 854 (1963).
[3]V. K. Shante and S. Kirkpatrick, Adv. Phys. **20**, 235 (1971).
[4]C. M. Fortuin and P. W. Kasteleyn, Physica **57**, 536 (1971).
[5]R. B. Potts, Proc. Cambridge Philos. Soc. **48**, 106 (1952).
[6]A. B. Harris, T. C. Lubensky, W. K. Holcomb, and C. Dasgupta, Phys. Rev. Lett. **35**, 327 (1975).
[7]R. G. Priest and T. C. Lubensky, Phys. Rev. B **13**, 4159 (1976).
[8]M. J. Stephen, Phys. Rev. B **15**, 5674 (1977).
[9]For a detailed discussion of this point, see A. Houghton, J. S. Reeve, and D. J. Wallace, Phys. Rev. B **17**, 2956 (1978).
[10]See, for example, S.-K. Ma, *Modern Theory of Critical Phenomena* (Addison-Wesley, New York, 1976).
[11]J. Rudnick and G. Gaspari, J. Stat. Phys. **42**, 833 (1986).
[12]In addition to Refs. 6, 7, and 8, see also G. R. Golner, Phys. Rev. B **8**, 3419 (1973); R. K. Zia and D. J. Wallace, J. Phys. A **8**, 1495 (1975).
[13]S. Kirkpatrick, Phys. Rev. Lett. **36**, 69 (1976).
[14]P. C. Martin, E. D. Siggian, and H. A. Rose, Phys. Rev. A **8**, 423 (1973).
[15]L. D. Faddev and V. N. Popov, Phys. Lett. **25B**, 29 (1967).
[16]*Handbook of Mathematical Functions,* edited by M. Abramowitz and I. Stegun (Dover, New York, 1970).
[17]M. E. Fisher, in *Critical Phenomena, Proceedings of the 1970 Enrico Fermi International School of Physics,* edited by M. S. Green (Academic, New York, 1971), Vol. 51. For a recent summary of finite-size results, see *Finite Size Scaling and Numerical Simulation of Statistical Systems,* edited by V. Privman (World Scientific, London, 1990).
[18]See, for example, E. Brézin and J Zinn-Justin, Nucl. Phys. **B257**, 867 (1985); J. Rudnick, H. Guo, and D. Jasnow, J. Stat. Phys. **41**, 353 (1985).
[19]V. Privman and M. E. Fisher, Phys. Rev. B **30**, 322 (1984).
[20]V. Privman, in *Finite Size Scaling and Numerical Simulation of Statistical Systems,* edited by V. Privman (World Scientific, London, 1990), pp. 1–98.